

Isotropic emission components in splintering central collisions: (17–115)A MeV $^{40}\text{Ar} + \text{Cu, Ag, Au}$

Rulin Sun,¹ E. Colin,^{1,4} N. N. Ajitanand,¹ John M. Alexander,¹ M. A. Barton,³ P. A. DeYoung,³ K. L. Drake,³
A. Elmaani,^{1,*} C. J. Gelderloos,^{6,†} E. E. Gualtieri,² D. Guinet,⁴ S. Hannuschke,² J. A. Jaasma,³ L. Kowalski,⁵ Roy A. Lacey,¹
J. Lauret,¹ E. Norbeck,⁷ R. Pak,² G. F. Peaslee,³ M. Stern,⁴ N. T. B. Stone,² S. D. Sundbeck,³ A. M. Vander Molen,²
G. D. Westfall,² L. B. Yang,⁷ and J. Yee²

¹Department of Chemistry, State University of New York at Stony Brook, Stony Brook, New York 11794

²National Superconducting Laboratory, Michigan State University, East Lansing, Michigan 48824

³Departments of Chemistry and Physics, Hope College, Holland, Michigan 49423

⁴Institut de Physique Nucléaire de Lyon, Institut National de Physique Nucléaire et de Physique des Particules–Centre National de la Recherche Scientifique/Université Claude Bernard, 43, Blvd. du 11 Novembre 1918, F-69622 Villeurbanne, Cedex, France

⁵Department of Physics and Geoscience, Montclair State College, Upper Montclair, New Jersey 07043

⁶Nuclear Physics Laboratory, University of Colorado, Boulder, Colorado 80309-0446

⁷Department of Physics and Astronomy, University of Iowa, Iowa City, Iowa 52242

(Received 8 November 1999; published 2 May 2000)

The ensemble of charged isotropically emitted ejectiles is studied for central collisions of (17–115)A MeV $^{40}\text{Ar} + \text{Cu, Ag, Au}$. Measurements of average multiplicities, spectral slopes, and masses of the heaviest fragments are compared to statistical models for multifragmentation or sequential evaporation. The multifragmentation models predict much more complete nuclear disassembly than is observed. The evaporation model reproduces the data much more closely except for the spectra of $Z=1$ ejectiles. The kinetic energies of $Z=1$ and 2 ejectiles are much less than found for 1A GeV $^{197}\text{Au} + ^{12}\text{C}$ for similar energy depositions. Entrance channel dynamics seem to affect the isotropic emission ensembles, often taken to define an equilibrated emission source.

PACS number(s): 25.70.Pq, 25.70.Hi

Central collisions between mass asymmetric heavy nuclei at near-barrier energies ($\leq 10A$ MeV) generally lead to excited compound nuclei. These compound nuclei can be rather well characterized by entrance-channel mass, charge, and energy because preequilibrium emission is not very prominent. The equilibrium emission from these systems is identified by its “isotropic” emission (or more properly, forward-backward symmetry in the frame of the emission source) [1]. A major objective of intermediate energy heavy ion reactions is to continue the characterization and study of the properties of hot composite nuclei to higher excitation energies and, in particular, to energies that lead to nuclear disassembly. Statistical or equilibrium models have been developed for nuclear decay that leads to multifragmentation for nuclear temperatures of ≥ 4 MeV [2,3] and to sequential pairwise decay (or evaporation) at lower temperatures [4]. Comparison of measurements to such model calculations provides the means to assign values to the thermodynamic properties of the hot nuclei produced.

A practical problem for intermediate energy ($\geq 15A$ MeV) reactions is the increasing probability for preequilibrium (or dynamical) emission and hence its separation from the equilibrium emission is quite important [5]. In recent work on the reactions $^{40}\text{Ar} + \text{Cu, Ag, Au}$, we have studied heavy fragments along with charged ejectiles in 4π sr [6,7].

The ejectiles have been separated into isotropic and forward-focused components. Isotropic emission in the moving frame of the heaviest fragment can be associated *a priori* with equilibrium emission from a very hot initial nucleus. Below we will comment on this point *a posteriori*. Forward directed emission can be associated with a preequilibrium spray from incomplete fusion and/or from splintering central collisions [5–8]. Here we discuss properties of the isotropic emission ensemble; in another paper we discuss the forward-peaked emission components [8].

The Michigan State University K1200 cyclotron delivered ^{40}Ar beams from (8–115)A MeV, i.e., from near barrier to well above fermi energies. The MSU 4π array provided both a multiplicity filter and an event by event list of angles, energies, and identities for the charged particles, and fragments [9]. Along with the basic “soccerball” array from $\sim 18^\circ$ to $\sim 162^\circ$, three forward-angle detection devices were used: (a) the zero degree detector (ZDD), a ring of eight plastic telescopes covering polar angles of $\sim 0.5^\circ$ to 1.5° [10], (b) the Maryland forward array (MFA), a second ring of plastic telescopes from 1.5° to 3° [11], and (c) a set of 45 Si detectors ($\sim 3\text{ cm} \times 3\text{ cm} \times 140\ \mu\text{m}$) [8,12] mounted ≈ 70 cm from the target in front of the 45 telescopes ($\sim 3^\circ$ to 18°) of the high rate array (HRA) [9]. Ionization chamber ΔE detectors were also used from 18° to 162° in front of each of the 170 telescopes in the ball [9]. Data from the plastic and gas detectors were recorded as described elsewhere [13], but only if two or more telescopes fired in the ball. In addition, energy and time-of-flight signals were recorded from each Si wafer. The data from these Si detectors were corrected for pulse height defect [14] and analyzed to give masses (resolution $\pm 5 - 10\%$) for the slow moving fragments ($A \geq 10$), while data from the other telescopes were analyzed to give atomic num-

*Present address: Battelle Pacific Northwest National Laboratory, National Security Division, Box 999, K6-48, Richland, WA 99352.

†Present address: Hughes Space and Communications, P.O. Box 92919, Los Angeles, CA 90009.

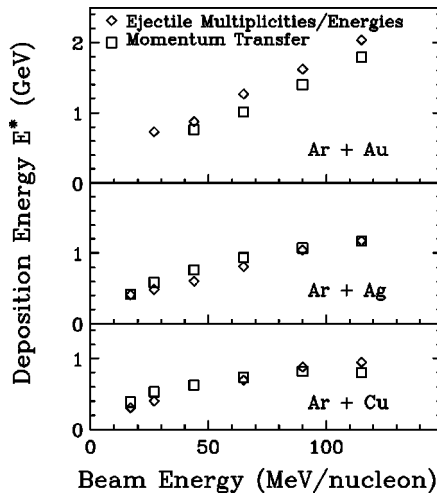


FIG. 1. Deposition energy for isotropic emission vs ^{40}Ar beam energy: squares from LMT values [6], diamonds from reconstruction of the isotropic emission ensemble [7]. Overall errors are $\sim 15\%$.

bers and energies for fragments of $Z \sim 1-8$ [9,15]. Following Refs. [6,7] we select those reactions with multiplicities in the highest 15% of those recorded; we also require that each selected event have a total detected charge ≥ 0.75 ($Z_{\text{target}} + Z_{\text{projectile}}$) and a total longitudinal momentum ≥ 0.70 ($P_{\text{projectile}}$).

Many properties of the observed heavy fragments have been presented and discussed in Refs. [6,7]. In particular, the average linear momentum transfer (LMT) was used to estimate the energy deposited into the remaining hot nuclear system. These estimated deposition energies are shown as squares in Fig. 1.

Also many properties of the light charged particles (LCPs) and intermediate mass fragments (IMFs) have been presented and discussed [7]. In particular, these ejectiles were separated into forward-focused and isotropic emission components. The average mass, energy, and longitudinal momentum carried by these two components were determined and systematized. Average energies of the isotropic emission ensemble were summed to reconstruct the initial deposition energy as shown by diamonds in Fig. 1. The general consistency of these two methods gives a good check on these average deposition energies.

For model calculations of hot nuclear decay, the deposition energy is an essential input. Also required is the initial mass and charge of the excited system. These quantities have also been obtained from systematic results on the ejectile multiplicities given in [7]. This is the most extensive set of reaction systems to date that have been so characterized.

For the span of nuclear excitations shown in Fig. 1, one expects that two-body sequential decays (nuclear evaporation) will dominate at the lower energies but then yield to multibody breakups (multifragmentation) at the higher energies. Figure 2 shows data and model calculations for the average mass of the heaviest remaining fragment (HF). These calculated results are not very sensitive to the widths of assumed distributions about the average input values. The two multifragmentation models [2,3] agree with one another

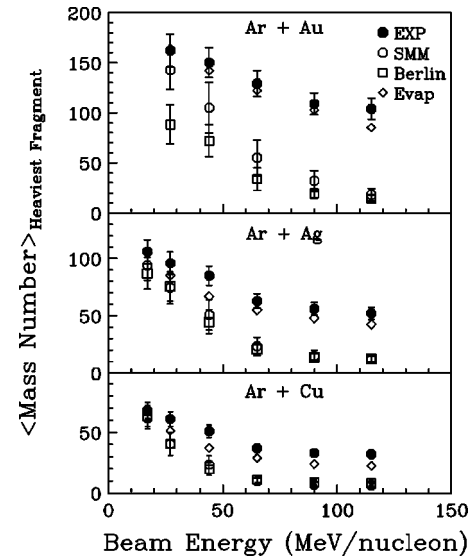


FIG. 2. Average mass of the heaviest fragment from experiment (closed circles) and calculations from the Copenhagen model (open circles), the Berlin model (squares), and sequential evaporation model (diamonds). Errors are $\sim 10\%$.

(except for Ar + Au at the lower energies where the Berlin model allows binary fission). These multifragmentation model calculations are consistent with the data at the lowest energies (allowing for binary fission in the Berlin model) but give much smaller HF masses at the higher energies.

By contrast the evaporation model [4] tracks the data very well with only slightly lower average mass predictions. Evidently, the multifragmentation models invest much more energy in nuclear disassembly or bond breakage compared to the evaporation model. Each calculation must conserve energy; therefore, the latter model must be investing more energy in kinetic energy of the ejectiles and less in nuclear disassembly.

Figure 3 shows average ejectile multiplicities divided into two categories LCPs ($Z=1,2$) and IMFs ($Z=3-18$) (both

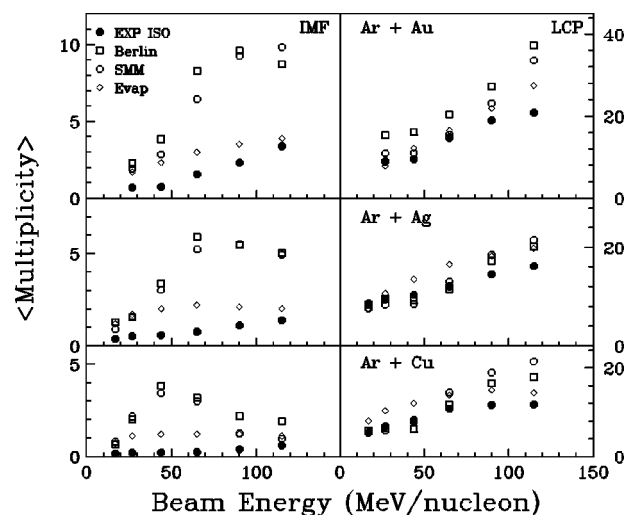


FIG. 3. Average multiplicities of IMFs (left) and LCPs (right). Symbols as in Fig. 2. Overall errors are $\sim 15\%$.

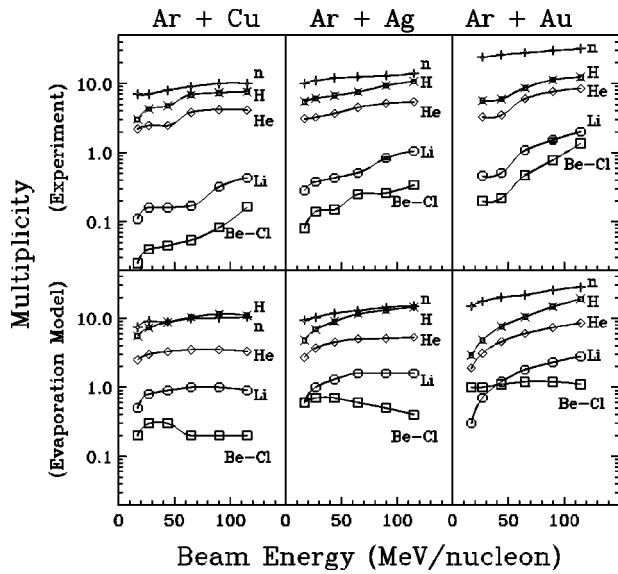


FIG. 4. Top panels show average multiplicities of charged ejectiles from this work and neutrons from systematic extrapolations. Lower panels show sequential evaporation model calculations. Overall errors are $\sim 15\%$.

isotropically emitted). The multifragmentation models dramatically overpredict the IMF multiplicities for these reactions; their IMF excitation functions also exhibit maxima at ~ 100 , 70 , and 50 A MeV for Au, Ag, and Cu, respectively. These maxima are related to the onset of so-called nuclear vaporization, i.e., the growing instability of IMFs with respect to lighter particle formation as the nuclear temperature is increased. Indeed, on close inspection one can see that the calculated LCP multiplicity values seem to increase more rapidly when the IMF values saturate or decrease. The data exhibit none of these features of multifragmentation. The evaporation model predicts smaller IMF multiplicities with points much closer to the data.

Figure 4 shows a more detailed display of multiplicity excitation functions for the data compared to sequential evaporation calculations [4]. The multiplicities for the light particles ($A \leq 4$) are in reasonable accord with the data. Both the data and the calculations show rather small multiplicities for Li and for Be-Cl, so these fragments do not have a major role in the decay patterns. A similar result was obtained for reactions induced by antiprotons [16]. It is interesting that the evaporation model represents these general aspects of the data pattern even though it has been generally expected to fail for the higher energies.

Figure 5 shows spectral shapes at high energies from data and from evaporation calculations [4] for $Z=1$ and $Z=2$ ejectiles ($\theta_{\text{lab}} \approx 93^\circ$). The characteristic exponential fall off has been parameterized by fitting with the traditional Maxwellian form $P(E) \propto (E-B) \exp(-E/s)$, where the spectral slope parameter is s . Figure 6 shows these empirical slope parameters for the data compared to values obtained from evaporation calculations [4] (by the same procedure). The calculations account for the slopes of the spectra for the $Z=2$ ejectiles for all energies, but for $Z=1$ ejectiles only at the lowest incident energies. One may conclude from Figs.

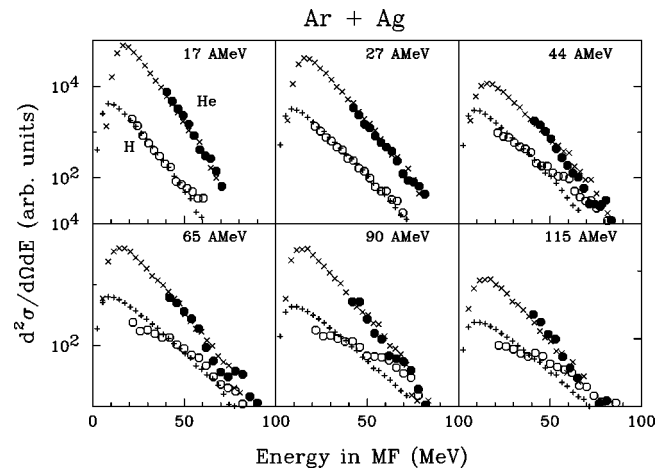


FIG. 5. Spectra ($\theta_{\text{lab}} \approx 93^\circ$) of $Z=1$ and $Z=2$ ejectiles in the moving frames. Data points are shown as circles and evaporation calculations (normalized) as crosses.

4–6 that the He emission is reasonably well described by evaporation from a thermalized system. The very high values of the slopes (or kinetic temperatures) for $Z=1$ ejectiles in Fig. 6 indicate a significant amount of extra thermal energy for H emission especially for incident energies of ≥ 65 A MeV. This back-angle emission cannot be assigned to the breakup of a projectilelike fragment.

It is interesting to compare these results for H and He from ^{40}Ar reactions ($E_{\text{c.m.}} \sim 3-4$ GeV) to similar results from $^{197}\text{Au} + ^{12}\text{C}$ ($E_{\text{c.m.}} \sim 12$ GeV) [17]. The isotropic energy removal and initial source masses for these two studies have a considerable overlap, here $9-13$ MeV/nucleon for $A_c \sim 210$ (Au), ~ 115 (Ag), or ~ 65 (Cu), compared to 12 ± 2 MeV/nucleon for $A_c \sim 130$ from 1A GeV Au + C [17]. If radial flow is mainly driven by excitation energy [18] and if all essential degrees of freedom are equilibrated, then the isotropic emission patterns should be very similar. In other words, details of the dynamical paths of excitation should be forgotten, and these studies should give similar results. Both

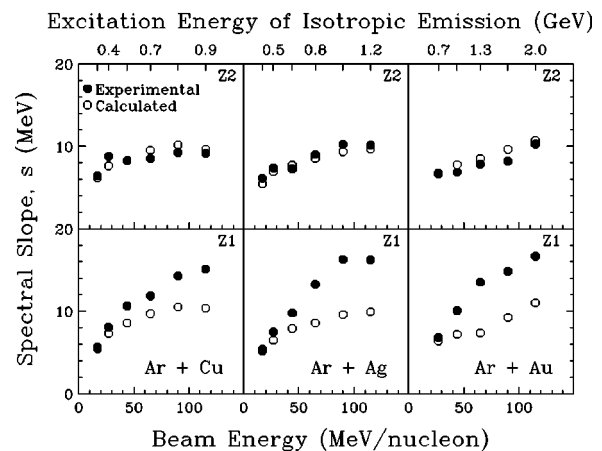


FIG. 6. Spectral slopes (i.e., kinetic temperatures) for $Z=1$ and $Z=2$ ejectiles at $\theta_{\text{lab}} \approx 93^\circ$ (observed and calculated). Errors from calibrations and statistics are $\sim 10\%$. Calculated values are from an evaporation model.

studies do reveal significant extra thermal energy (possibly radial flow) especially for the light ejectiles ($Z=1$) but the magnitudes are quite different. For ^{40}Ar reactions the extra thermal energy is apparent only for H emission, but not for He. For Au + C a substantial extra thermal energy was found for H, He, and even larger Z values. In particular, the average kinetic energies for isotropically emitted He are ~ 65 MeV for 1A GeV Au + C compared to ~ 28 MeV for 115A MeV Ar + Ag. The average kinetic energy difference for emission of H ejectiles is also ~ 60 MeV.

The vastly different kinetic energies indicate that equilibration of all relevant degrees of freedom has not occurred for both sets; there must remain some dynamic driving force that produces a much higher fraction of radial expansion or preequilibrium energy for the reaction 1A GeV Au + C. Evidently for the highly excited nuclear systems formed by Ar + Cu, Ag, Au, the dynamical evolution follows a very different path from Au + C, even though the total deposition energies are quite similar. Dynamical BUU model calculations indicate a significant difference in the localization of the deposition energy due to the differences in the mass asymmetry and the pace of the reactions [17,19].

The obvious difference is the nucleon-nucleon c.m. energy. A major path for energy deposition in 1A GeV Au + C collisions is resonance and meson creation [20], but one would expect only mild compression of the nuclear material. By contrast, there is very little meson or resonance production for 115A MeV ^{40}Ar reactions, but they should generate

substantial density compression possibly followed by expansion to forms that might resemble bubbles or doughnuts [21]. In fact, the BUU model calculations predict an oscillating core nuclear volume for the Ar reactions compared to one continuous volume expansion for Au + C [17]. At these high deposition energies, a substantial fraction of the lighter ejectiles may well depart before the collective motions and nuclear shapes can equilibrate [22].

In summary, we have studied the isotropic emission ensemble and the masses of the heaviest remaining fragments in central collisions of ^{40}Ar [(17–115)A MeV]. Results have been compared to calculations for multifragmentation and evaporation models. The multifragmentation models predict more extensive nuclear disassembly and IMF emission than is observed. The general features of the data are accounted for reasonably well by the sequential evaporation model even for core nuclear excitation of up to 10 MeV/nucleon where multifragmentation or vaporization is generally expected. Less extra thermal energy is found here for the $Z=1$ and 2 ejectiles, than that found elsewhere for the reaction 1A GeV Au + ^{12}C [17]. It seems that even the isotropic emission components are significantly affected by entrance channel dynamics, which challenges the simple notion of equilibration.

Financial support has been provided by the U.S. Department of Energy, the National Science Foundation, and the CNRS of France.

-
- [1] D. Logan *et al.*, Phys. Rev. C **22**, 1080 (1980).
 - [2] D. H. E. Gross, Rep. Prog. Phys. **53**, 605 (1990).
 - [3] J. P. Bondorf *et al.*, Phys. Rep. **257**, 133 (1995).
 - [4] Our calculations use the code described by N. N. Ajitanand *et al.*, Nucl. Instrum. Methods Phys. Res. A **376**, 213 (1996).
 - [5] M. T. Magda *et al.*, Phys. Rev. C **53**, R1473 (1996).
 - [6] E. Colin *et al.*, Phys. Rev. C **57**, R1032 (1998).
 - [7] R. Sun *et al.*, Phys. Rev. Lett. **84**, 43 (1999).
 - [8] R. Sun *et al.*, Phys. Rev. C (submitted).
 - [9] G. D. Westfall *et al.*, Nucl. Instrum. Methods Phys. Res. A **238**, 347 (1985); M. Maier *et al.*, *ibid.* **337**, 619 (1994); A. M. Vander Molen *et al.*, IEEE Trans. Nucl. Sci. **41**, 80 (1994); R. Pak, Ph.D. thesis, Michigan State University, 1996.
 - [10] N. T. B. Stone, Ph.D. thesis, Michigan State University, 1996.
 - [11] D. E. Russ, Ph.D. thesis, University of Maryland, 1996.
 - [12] Detectors on loan from Technische Universitat, Darmstadt; E. Berthoumieux *et al.*, Phys. Rev. C **57**, 1788 (1998).
 - [13] W. J. Llope *et al.*, Phys. Rev. C **52**, 1900 (1995).
 - [14] J. B. Moulton *et al.*, Nucl. Instrum. Methods Phys. Res. A **157**, 325 (1978).
 - [15] D. A. Cebra *et al.*, Nucl. Instrum. Methods Phys. Res. A **300**, 518 (1991).
 - [16] U. Jahnke *et al.*, Phys. Rev. Lett. **83**, 4959 (1999).
 - [17] J. Lauret *et al.*, Phys. Rev. C **57**, R1051 (1998).
 - [18] D. Durand, LPC Caen Report No. LPC C98-02, 1997, and references therein.
 - [19] Our calculations use the code described by P. Danielewicz, Phys. Rev. C **51**, 716 (1995).
 - [20] R. Averbeck *et al.*, Z. Phys. A **359**, 65 (1997); nucl-ex/9803001.
 - [21] N. T. B. Stone *et al.*, Phys. Rev. Lett. **78**, 2084 (1997); E. Norbeck *et al.*, Nucl. Phys. **A607**, 105 (1996).
 - [22] Ph. Endes *et al.*, Phys. Rev. C **56**, 2003 (1997); F. Haddad *et al.*, *ibid.* **60**, 031603 (1999).